

Cross section measurements using gas and solid targets for production of the positron-emitting radionuclide O-14

By Z. Kovács^{1,2}, B. Scholten^{1,2}, F. Tárkányi^{1,2}, H. H. Coenen¹ and S. M. Qaim^{1,*}

¹ Institut für Nuklearchemie, Forschungszentrum Jülich GmbH, D-52425 Jülich, Germany

² Institute of Nuclear Research of the Hungarian Academy of Sciences, H-4001 Debrecen, Hungary

(Received July 22, 2002; accepted in revised form October 1, 2002)

*N₂ gas target / Nitrogen-containing solid target /
Nuclear reaction / Excitation function / Thick target yield /
Positron emitters ¹¹C, ¹³N, ¹⁴O / PET*

Summary. Irradiation of nitrogen with protons leads to ¹¹C ($T_{1/2} = 20.4$ min) via the well-known ¹⁴N(p, α) reaction. However, ¹⁴O ($T_{1/2} = 70.6$ s) and ¹³N ($T_{1/2} = 10$ min) are also formed as side products via the ¹⁴N(p, n) and ¹⁴N($p, d + pn$) reactions, respectively. In this work detailed cross section measurements were carried out for those two side reactions up to 19.2 MeV using N₂ gas and nitrogen-containing solid targets. From the data, the thick-target yields and the exact level of radioactive impurities in ¹¹C were calculated. In the case of ¹⁴O, the results also confirmed the possibility of producing this β^+ emitting radionuclide in sufficient quantities for PET investigations.

1. Introduction

The radionuclide ¹¹C ($T_{1/2} = 20.4$ min) is widely used for preparing radiopharmaceuticals for Positron Emission Tomography (PET). It is generally produced via the ¹⁴N(p, α)¹¹C reaction. However, appreciable amounts of two other positron emitters, viz. ¹⁴O ($T_{1/2} = 70.6$ s) and ¹³N ($T_{1/2} = 10$ min) are also formed as side products via the ¹⁴N(p, n)¹⁴O and ¹⁴N($p, d + pn$)¹³N reactions, respectively. In the first few minutes after the end of bombardment (EOB), these short-lived products can considerably increase the level of radioactivity in the batch. The decay data of the three radionuclides concerned are given in Table 1 [1].

It is especially important to know the ¹⁴O and ¹³N contamination levels when continuous ¹¹CO or ¹¹CO₂ production and inhalation combined with PET investigations are considered. The shorter-lived ¹⁴O has also recently been suggested as a substitute for the commonly used ¹⁵O ($T_{1/2} = 2.0$ min) in PET studies [2, 3]. A yet another application of ¹⁴O is emerging. The radionuclide produced is chemically separated and fed in an ion source to produce a radioactive ¹⁴O beam for astrophysics research [4]. The hitherto available cross section database for the formation of both ¹⁴O and ¹³N [cf. 5–12], however, is not complete enough

to allow calculation of the exact yields. In this work, excitation functions were measured and integral yields calculated for all the three above mentioned reactions. Studies on ¹¹C were performed only to check the accuracy of the techniques used; the emphasis was on the formation of ¹⁴O and ¹³N.

2. Experimental

2.1 Gas cells and thin solid samples

Stainless steel gas cell cylinders (2 cm diameter, 2.5 cm length), having 50 μ m thick Al windows were used. They were filled with natural nitrogen gas (Linde AG, Germany, 99.9999%) at a pressure of about 2 bar. The gas cell evacuating and filling station was the same as described earlier [13]. Additionally, boron nitride (BN) solid samples were prepared from a rod (hot pressed, 12.7 mm diameter, 100 mm length), supplied by Goodfellow Metals, Cambridge, England, by cutting it into about 0.2 mm thick discs. For degradation of the incident proton energies Al foils (supplied by Goodfellow Metals, Cambridge, England) of different thicknesses (50–700 μ m) were used.

2.2 Irradiations

Irradiations were performed at the compact cyclotron CV 28 in Jülich. The primary incident proton energies were 12, 16 and 20 MeV. In all irradiations the charged particle beam flux was measured with a Faraday cup as well as via monitor reactions induced in copper foils (^{nat}Cu(p, xn)⁶³Zn and ^{nat}Cu(p, xn)⁶²Zn processes) [14] placed both in front and at the back of each gas cell and solid sample. For ¹⁴O cross section measurements, each gas target chamber was individually irradiated. Additionally, six thin solid BN samples were also irradiated individually. For ¹³N cross section measurements, 5 stacked gas chambers were irradiated at the same time. All irradiations were performed with beam currents of 30–170 nA for 3 minutes.

The effective charged particle energy in each monitor foil, BN target and gas cell was obtained via calculation [15] using the exact thickness and isotopic composition of the elements along the degraded beam.

* Author for correspondence (E-mail: s.m.qaim@fz-juelich.de).

Table 1. Decay properties of the product nuclei formed in the interactions of protons with ^{14}N .

Nuclide	Half-life	Mode of decay (%)	E_{β^+} [MeV]	E_{γ} [keV]	I_{γ} [%]
^{11}C	20.39 min	β^+ (99.8) EC(0.2)	0.96		
^{13}N	9.96 min	β^+ (100)	1.20		
^{14}O	70.6 s	β^+ (100)	1.81 (99.4%) 4.12 (0.6%)	2312.7	99.4

2.3 Measurement of radioactivity

The radioactive products formed in the gas cells, solid targets and monitor foils were measured *via* high-resolution gamma ray spectroscopy using well-calibrated HPGe-detectors. Each sample was measured at a large detector-sample distance to avoid corrections for the extended nature of the source and to reduce pile-up and coincidence losses. In the case of ^{14}O , the 2312.7 keV γ -ray was assayed. The first measurement of each sample was started within 1 minute after EOB. Each sample was measured consecutively 4 times for 1 minute to follow the decay.

An important aspect of this measurement was the calibration of the detector. For γ -ray energies up to 2 MeV, standard sources (supplied by the PTB Braunschweig) were used. For higher energies a self-prepared ^{24}Na point source, calibrated *via* its 1369 keV γ -ray, was used. Its 2754 keV γ -ray served as a reference point for efficiency calibration.

In the case of ^{13}N , the decay of the 511 keV γ -ray was followed. The five simultaneously irradiated gas cells were measured one after another and the measurements were successively repeated 11 more times, until at least 4 such points were obtained for the decay of ^{11}C where the activity of the ^{13}N became negligible. Two series of five gas cells were irradiated and measured, thus giving ten points for each cross section curve.

2.4 Data analysis

From the known total number of nitrogen nuclei, the measured activities and beam intensities, cross sections were calculated using the standard activation formula. The decay data employed to convert count rates into decay rates are given in Table 1 [cf. 1].

No special correction was made for the response function of the HPGe-detector because of the extended source character of the target gas cell and for a possible non-uniform distribution of the adsorbed activity on the inner walls of the target. In view of the target to detector distance of around 50 cm, those two effects should be negligible. The number of target nuclei in each cell was determined from the geometrical dimensions of the target, the isotopic composition and pressure of the gas, and the actual temperature. Since low current irradiations were involved, no special correction was made for the gas density reduction effect.

The results of direct beam current measurements showed good agreement with those obtained *via* monitor reactions. The difference was generally low, reaching a maximum of 10% only in a few cases.

The uncertainty in each cross section was determined as described in several earlier publications [cf. 16]. The uncertainties of the contributing processes were estimated as

follows: absolute activity (7%–12%), beam current (10%), decay data used (3%), number of target nuclei (5%–10%). The resulting uncertainty of the cross section was calculated by a quadratic summation of the individual values; it was found to be 15%–20%. The calculated cross sections for the $^{14}\text{N}(p, n)^{14}\text{O}$, $^{14}\text{N}(p, \alpha)^{11}\text{C}$ and $^{14}\text{N}(p, d + pn)^{13}\text{N}$ nuclear reactions are given in Table 2. They are based on two independent measurements: in the case of ^{14}O , short irradiation

Table 2. Cross sections of $^{14}\text{N}(p, n)^{14}\text{O}$, $^{14}\text{N}(p, \alpha)^{11}\text{C}$ and $^{14}\text{N}(p, pn)^{13}\text{N}$ reactions.

Proton energy (MeV)	Cross section [mb]		
	$^{14}\text{N}(p, n)^{14}\text{O}$	$^{14}\text{N}(p, \alpha)^{11}\text{C}$	$^{14}\text{N}(p, d + pn)^{13}\text{N}$
6.4 ± 0.5	0.003		
6.4 ± 0.6	0.01		
7.0 ± 0.5	2.7 ± 0.6		
7.0 ± 0.5	2.8 ± 0.4		
7.6 ± 0.5	4.9 ± 0.9		
7.7 ± 1.1 ^a	5.2 ± 0.9		
7.7 ± 0.4	6.2 ± 0.7		
8.0 ± 0.4	7.0 ± 1.0		
8.2 ± 0.3	7.9 ± 0.7		
8.5 ± 0.3	6.1 ± 0.7		
9.0 ± 0.3	5.7 ± 0.6		
9.2 ± 0.4	5.3 ± 0.5		
9.5 ± 0.2	5.7 ± 0.6		
9.9 ± 0.2	8.5 ± 0.6		
10.2 ± 1.0 ^a	6.9 ± 0.5		
10.4 ± 0.2	4.5 ± 0.8		
10.6 ± 0.2	5.2 ± 1.0		
10.7 ± 0.2	3.8 ± 0.5		
10.8 ± 0.7	4.3 ± 0.8		
11.4 ± 0.5		127 ± 16	3 ± 0.8
11.7 ± 0.6	2.2 ± 0.4		
12.1 ± 0.4		91 ± 14	6 ± 1.5
12.2 ± 0.5 ^a	4.7 ± 0.7		
12.8 ± 0.4	5.5 ± 1.0		
12.9 ± 0.5	7.0 ± 1.3		
13.1 ± 0.3		110 ± 14	17 ± 3
13.5 ± 0.3 ^a	6.3 ± 0.6		
13.9 ± 0.2	5.0 ± 0.7		
14.1 ± 0.2		113 ± 15	26 ± 4
15.0 ± 0.2	2.9 ± 0.5		
15.1 ± 0.2		86 ± 11	29 ± 4
15.4 ± 0.2	3.9 ± 0.5		
15.5 ± 0.6		92 ± 12	24 ± 3
15.8 ± 1.0 ^a	3.1 ± 0.4		
16.5 ± 0.4		75 ± 10	22 ± 3
17.4 ± 0.3		66 ± 9	31 ± 4
17.5 ± 0.4	3.1 ± 0.4		
18.3 ± 0.2		52 ± 7	39 ± 5
18.6 ± 0.2 ^a	2.4 ± 0.4		
19.1 ± 0.2	2.9 ± 0.4		
19.2 ± 0.2		53 ± 10	40 ± 5

a: BN targets, the others were N_2 filled gas cells.

followed by γ -ray spectrometry was used. For ^{13}N and ^{11}C , longer irradiation followed by an analysis of the 511 keV peak was utilized.

The uncertainty in the effective projectile energy was estimated by taking into account the inhomogeneities of the target elements. Typical estimated uncertainty of the mean energy was around ± 0.2 MeV for the front cell of the stack or for single cell without energy absorber. At the last cell in a stack of five cells, or for a single cell with 6–700 μm Al absorber in front, it reached up to ± 1.7 MeV. The uncertainties in proton energy are given in Table 2.

3. Results and discussion

3.1 Excitation functions

3.1.1 $^{14}\text{N}(p,n)^{14}\text{O}$ reaction

For the $^{14}\text{N}(p,n)^{14}\text{O}$ reaction, 25 cross section data points were obtained using N_2 gas targets and additional 6 from BN targets. The energy range covered was from threshold ($E = 6.4$ MeV) up to 19.1 MeV. The solid targets were easier to handle, but had the disadvantage of being thicker (the energy degradation was 1.1 to 2.0 MeV instead of 0.3 to 0.5 MeV in the gas cells), resulting in a lower resolution of the fine structure of the excitation function curve than in the case of gas targets. The data obtained from both methods, however, agree within their uncertainties. The results are shown in Fig. 1 together with the available literature data.

In the literature, five series of measurements have been described. The measurements of Kuan and Risser [5] (from threshold to 12 MeV) were the first on this subject but their cross sections are at least ten times higher than the values in other works. Therefore, the curve in Fig. 1 is shown in 1/10 multiplication for better comparison. Nozaki and Iwamoto [6] reported a curve from threshold up to 15 MeV and Dyer *et al.* [7] gave numerical data over the energy range of 7 to 20 MeV. All the measurements generally show a broad resonance at about 8 MeV and a sharper maximum at 10 MeV. The shapes of the three excitation function curves are similar below 10.5 MeV but not the absolute magnitudes. Above this energy the data of Kuan and Risser rise strongly

while those of Nozaki and Iwamoto as well as of Dyer *et al.* decrease at first and then again show a weak peak around 13.5 MeV.

An eye-guide curve through our data points shows the first maximum at 8.2 MeV. The second and the third maxima at 9.9 and 13.1 MeV, respectively, are also reproduced. In general, our values follow the trend given by Nozaki and Iwamoto [6] as well as by Dyer *et al.* [7], but the magnitudes are generally 10 to 20% lower. Besides the three above mentioned works, in the energy region above 12 MeV a few data points have been reported by Kitwanga *et al.* [8]. Except for the cross section value at 12 MeV, where our point is much lower, there is a good agreement. It is interesting to mention that in another work, Muminov *et al.* [9] reported data on this reaction for three energy points between 6.85 and 11.0 MeV. Those points are also given in 1/10 multiplication in Fig. 1; they show a correlation with the curve of Kuan and Risser [5] and are presumably also wrong.

We recently presented a preliminary report on this reaction [17]. The present data are based on a more accurate analysis. A small peak at 7.3 MeV was previously observed due to some energy shift. This has now disappeared. The remaining resonance structure in the excitation function can be understood in terms of the excitation energy of the intermediate nucleus [$^{15}\text{O}^*$] and the level structure of the product nucleus ^{14}O . The eye-guide curve through our measured data points should now serve as a good base for calculating the yield of ^{14}O .

3.1.2 $^{14}\text{N}(p,\alpha)^{11}\text{C}$ reaction

The 10 measured cross section data points of the $^{14}\text{N}(p,\alpha)^{11}\text{C}$ reaction are shown in Fig. 2 together with a recommended curve recently published by the IAEA [18], which is based on an evaluation of 8 detailed excitation function measurements described in the literature. Our data are in good agreement with the recommended curve. This proves the reliability of the techniques used in this work. Moreover, as far as we know, over the energy region of 14.5 to 19.2 MeV, hitherto only one set of data by Jacobs *et al.* [10] has been reported. Our measurements thus strengthen the existing data base.

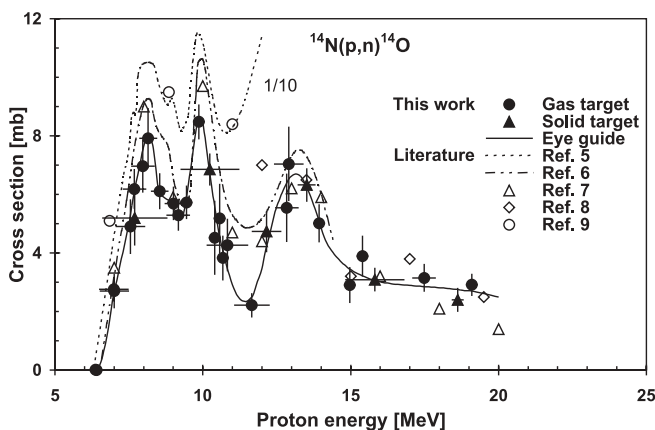


Fig. 1. Excitation function of the $^{14}\text{N}(p,n)^{14}\text{O}$ nuclear reaction. The data of Refs. [5] and [9] are shown in 1/10 multiplication.

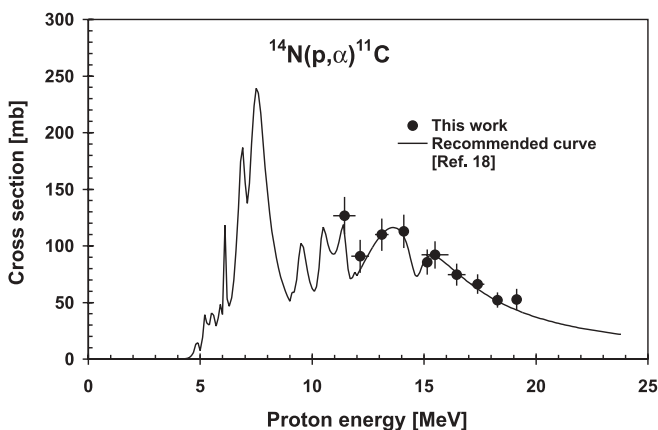


Fig. 2. Excitation function of the $^{14}\text{N}(p,\alpha)^{11}\text{C}$ nuclear reaction.

3.1.3 $^{14}\text{N}(p, d + pn)^{13}\text{N}$ reaction

For each energy value encountered in the study of the (p, α) reaction, the cross section was also deduced for the $^{14}\text{N}(p, d + pn)^{13}\text{N}$ reaction. The data points are shown in Fig. 3 for the energy range from 11.3 to 19.2 MeV. Since this reaction is not used for production purposes, so far it has not been studied in detail and only two series of data were found in the literature [11, 12]. Those are also shown in Fig. 3 for comparison.

Our cross section values show discrepancy with both the series. Up to the first maximum at about 15 MeV it follows the trend of the data of Muminov *et al.* [12], although our cross section values are higher. The excitation function of Sajjad *et al.* [11] shows no maximum at 15 MeV. Around 16.2 MeV our excitation function shows a small minimum and the cross section of 21.9 mb is in agreement with the two literature values within the limits of experimental errors. Beyond that energy the data in this work and those of Sajjad *et al.* [11] show an increase. However, at 19 MeV our data are about 20% higher. Muminov *et al.* [12] did not report any increase till about 18 MeV.

The shape of the excitation function of this process suggests that in the formation of ^{13}N several reaction channels are involved. We presume that in the energy region from threshold up to 15 MeV, the $^{14}\text{N}(p, d)^{13}\text{N}$ reaction is dominant and after 16.5 MeV, the $^{14}\text{N}(p, pn)^{13}\text{N}$ process becomes increasingly important.

3.2 Calculated yields

The thick target yields calculated from the excitation functions are shown in Fig. 4. For each reaction the calculation was done for a 5 minute activation and for saturation. In the case of ^{14}O , the two yield curves are practically the same because of its short half-life. The yield values calculated from the excitation curve of Nozaki and Iwamoto [6] are also shown in Fig. 4. Our values are 15%–20% smaller, obviously due to somewhat lower cross sections in our work as compared to Nozaki and Iwamoto.

From the curves given in Fig. 4 it can be concluded that in routine production of ^{11}C , where an irradiation time of 30–50 minutes is common, the radioactivity produced will

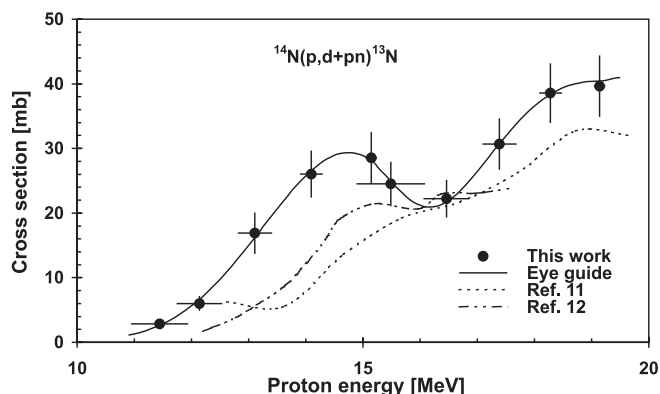


Fig. 3. Excitation function of the $^{14}\text{N}(p, d + pn)^{13}\text{N}$ nuclear reaction.

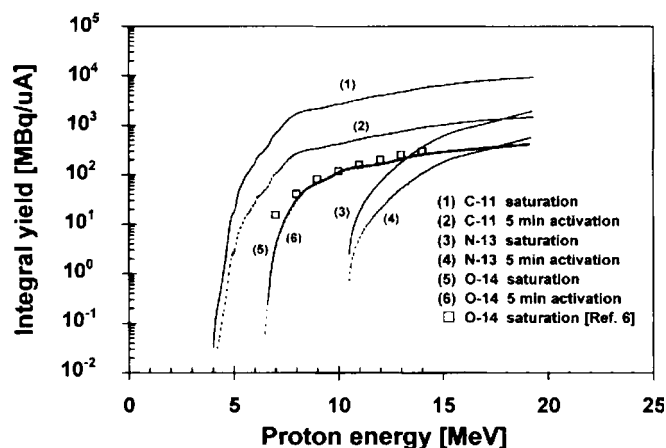


Fig. 4. Integral yields of ^{11}C , ^{13}N and ^{14}O via the $^{14}\text{N}(p, a)^{11}\text{C}$, $^{14}\text{N}(p, d + pn)^{13}\text{N}$ and $^{14}\text{N}(p, n)^{14}\text{O}$ nuclear reactions, respectively, for 5 minute activation and at saturation.

be about 92% ^{11}C and about 8% ^{14}O and ^{13}N . In case of short (1–3 minutes) irradiations, however, the level of contaminants may amount to 30% or more (at EOB). Because of the hard 2312 keV γ -line of the ^{14}O isotope, special shielding needs to be considered. In flow systems, where the activated gas is continuously carried away, the same problem occurs. In the latter case, calculations are necessary to determine the suitable length of the tube taking the gas to the place of inhalation so that the amount of ^{14}O is decreased by decay to an acceptable level.

As regards the possibility of routine production of ^{14}O , the calculated yield of about 370 MBq/ μA at a low energy cyclotron ($E_p < 18$ MeV) would ensure a supply of about 10 GBq activity under practical conditions. In a nitrogen gas target containing some oxygen, ^{11}C is formed predominantly as $^{11}\text{CO}_2$ and can be removed using a low temperature trap or, as described by Sajjad *et al.* [3], by passing through charcoal, soda lime and 5 Å molecular sieve traps. The ^{14}O remaining in the nitrogen gas exists as $^{14}\text{O}_2$. It may also be mentioned that the available synthesis methods for preparing labeled butanol or water are quick enough to allow replacing the ^{15}O isotope with the shorter-lived ^{14}O . During those syntheses the ^{13}N produced is eliminated to the waste-line.

4. Conclusion

Excitation function measurements and yield calculations on the $^{14}\text{N}(p, n)^{14}\text{O}$ and $^{14}\text{N}(p, d + pn)^{13}\text{N}$ nuclear reactions have provided the possibility to determine the contamination levels caused by these side reactions in the production of ^{11}C . At the same time detailed studies strengthened the data base for the $^{14}\text{N}(p, n)^{14}\text{O}$ nuclear reaction from its threshold till 19.1 MeV. The thick yield calculation shows that this positron emitting radionuclide can be produced in sufficient amounts for PET investigations.

Acknowledgment. This work was carried out under a German-Hungarian bilateral research agreement (Project No. in Germany HUN 27/98; in Hungary D-11/98) and we thank the concerned authorities for financial support. The authors thank the crew of the

compact cyclotron CV 28 for irradiations and F. Szelecsényi for a useful discussion.

References

1. Firestone, R. B.: *Table of Isotopes*. 8th Edition, Wiley, New York (1996).
2. Sajjad, M., Liow, J. S., Zaini, M. R., Rottenberg, D. A., Strother, S. C.: Fast PET scanning for brain activation studies with [¹⁴O]water. *J. Nucl. Med.* **5**, 244P (2000).
3. Sajjad, M., Zaini, M. R., Liow, J. S., Rottenberg, D. A., Strother, S. C.: Production and dosimetry of [¹⁴O]H₂O for PET activation studies. *Appl. Radiat. Isotopes* **58**, 69 (2003).
4. O'Neil, J. P., Ramsey, C. A., Powell, J., Cerny, J.: Targetry and chemistry for the production of ¹⁴O: Application to radioactive ion beam experiments. 9th Int. Workshop on Targetry and Target Chemistry, Turku, Finland, May 2002, Abstract E11.
5. Kuan, H. M., Risser, J. R.: Excitation function of the ¹⁴N(*p, n*)¹⁴O total cross section from threshold to 12 MeV. *Nucl. Phys.* **51**, 518 (1964).
6. Nozaki, T., Iwamoto, M.: Yield of ¹⁴O for the reactions ¹⁴N(*p, n*)¹⁴O, ¹²C(³He, *n*)¹⁴O and ¹²C(*α, 2n*)¹⁴O. *Radiochim. Acta* **29**, 57 (1981).
7. Dyer, P., Bodansky, D., Seamster, A. G., Norman, E. B., Maxson, D. R.: Cross section relevant to gamma-ray astronomy: Proton induced reactions. *Phys. Rev. C* **23**, 1865 (1981).
8. Kitwanga, S. wa, Leleux, P., Lipnik, P., Vanhovebeek, J.: Production of ^{14,15}O, ¹⁸F and ¹⁹Ne radioactive nuclei from (*p, n*) reactions up to 30 MeV. *Phys. Rev. C* **42**, 748 (1990).
9. Muminov, V. A., Muhamedov, S., Vasidov, A.: Possibilities of proton activation analysis using short-lived radioisotopes. *Atomnaja Energija* **49**, 101 (1980).
10. Jacobs, W. W., Bodansky, D., Chamberlein, D., Oberg, D. L.: Production of Li and B in proton and alpha particle reactions on ¹⁴N at low energies. *Phys. Rev. C* **9**, 2134 (1974).
11. Sajjad, M., Lambrecht, R. M., Wolf, A. P.: Cyclotron isotopes and radiopharmaceuticals XXXVII. Excitation functions for the ¹⁶O(*p, α*)¹³N and ¹⁴N(*p, pn*)¹³N reactions. *Radiochim. Acta* **39**, 165 (1986).
12. Muminov, V. A., Muhamedov, S., Sultanov, B., Khamrakulov, T.: Excitation functions of ¹⁴N(*p, α*)¹¹C and ¹⁴N(*p, pn*)¹³N nuclear reactions. *Izvestija Akademij Nauk Uzbeq SSR* 1974; Series of Physical-Mathematical Sciences **56** (1974).
13. Tárkányi, F., Qaim, S. M., Stöcklin, G.: Excitation functions of ³He-particle induced nuclear reactions on enriched ⁸²Kr and ⁸³Kr. *Radiochim. Acta* **43**, 185 (1988).
14. Tárkányi, F., Takács, S., Gul, K., Hermanne, A., Mustafa, M. G., Nortier, M., Oblozinsky, P., Qaim, S. M., Scholten, B., Shubin, Yu. N., Youxiang, Z.: Beam monitor reactions, in Charged Particle Cross-section Database for Medical Radioisotope Production: Diagnostic Radioisotopes and Monitor Reactions. Vienna, IAEA. IAEA-TECDOC-1211. (<http://www.nds.or.at/medical>) (2001) p. 49.
15. Williamson, C. F., Boujot, J. P., Picard, J.: Tables of Range and Stopping Power of Chemical Elements for Charged Particles of Energy 0.5 to 500 MeV. Report CEA-R 3042 (1966).
16. Hess, E., Takács, S., Scholten, B., Tárkányi, F., Coenen, H. H., Qaim, S. M.: Excitation function of the ¹⁸O(*p, n*)¹⁸F nuclear reaction from threshold up to 30 MeV. *Radiochim. Acta* **89**, 357 (2001).
17. Scholten, B., Hess, E., Takács, S., Kovács, Z., Tárkányi, F., Coenen, H. H., Qaim, S. M.: Cross section measurements relevant to the production of the positron emitting radionuclides ¹⁴O, ¹⁸F and ⁷⁶Br. *J. Nucl. Sci. Technol. Suppl.* **2** 1278 (August 2002).
18. Qaim, S. M., Tárkányi, F., Takács, S., Hermanne, A., Nortier, M., Oblozinsky, P., Scholten, B., Shubin, Yu. N., Youxiang, Z.: Positron emitters, in Charged Particle Cross-section Database for Medical Radioisotope Production: Diagnostic Radioisotopes and Monitor Reactions. Vienna, IAEA. IAEA-TECDOC-1211. (<http://www.nds.or.at/medical>) (2001) p. 234.